A Monovalent Mutant of Cyanovirin-N Provides Insight into the Role of Multiple Interactions with gp120 for Antiviral Activity[†,‡]

Raimund Fromme,[#,§] Zivile Katiliene,[#,§] Barbara Giomarelli,[||] Federica Bogani,[§] James Mc Mahon,[||] Toshiyuki Mori,[||,⊥] Petra Fromme,[§] and Giovanna Ghirlanda*[,§]

Department of Chemistry and Biochemistry, Arizona State University, Tempe, Arizona 85287-1604, and Center for Cancer Research, National Cancer Institute, NCI-Frederick, Frederick, Maryland 21702-1201

Received April 9, 2007; Revised Manuscript Received May 23, 2007

ABSTRACT: Cyanovirin-N (CV-N) is a 101 amino acid cyanobacterial lectin with potent antiviral activity against HIV, mediated by high-affinity binding to branched N-linked oligomannosides on the viral surface envelope protein gp120. The protein contains two carbohydrate-binding domains, A and B, each of which binds short oligomannosides independently in vitro. The interaction to gp120 could involve either a single domain or both domains simultaneously; it is not clear which mode would elicit the antiviral activity. The model is complicated by the formation of a domain-swapped dimer form, in which part of each domain is exchanged between two monomers, which contains four functional carbohydrate-binding domains. To clarify whether multivalent interactions with gp120 are necessary for the antiviral activity, we engineered a novel mutant, P51G-m4-CVN, in which the binding site on domain A has been knocked out; in addition, a [P51G] mutation prevents the formation of domain-swapped dimers under physiological conditions. Here, we present the crystal structures at 1.8 Å of the free and of the dimannose-bound forms of P51G-m4-CVN, revealing a monomeric structure in which only domain B is bound to dimannose. P51G-m4-CVN binds gp120 with an affinity almost 2 orders of magnitude lower than wt CV-N and is completely inactive against HIV. The tight binding to gp120 is recovered in the domain-swapped version of P51G-m4-CVN, prepared under extreme conditions. Our findings show that the presence of at least two oligomannoside-binding sites, either by the presence of intact domains A and B or by formation of domain-swapped dimers, is essential for activity.

Cyanovirin-N (CV-N[1]) is a small (11 kDa) lectin isolated from the cyanobacterium *Nostoc ellipsosporum* with potent virucidal activity against human immunodeficiency virus (HIV) (*1*) and other enveloped viruses (*2*−*4*); the protein is currently under investigation as a viral microbicide to prevent mucosal transmission of HIV (*5*, *6*). The antiviral activity is mediated via high-affinity interactions with the mannose-rich oligosaccharides linked to the viral surface envelope glycoproteins, such as HIV gp120 (*7*−*9*). This unique mode of action has spurred extensive structural and biophysical studies of the protein and its interaction with oligosaccharides as reviewed recently (*4*, *10*).

Several structures of CV-N and of its complexes with high-mannose carbohydrates have been determined by NMR (*11*, *12*) and X-ray crystallography (*13*, *14*). The solution structure (*12*) consists of a novel β-sheet fold that comprises two quasi-symmetric domains, A (residues 1−38/90−101) and B (residues 39−89), connected on each side by a short helical linker. Each domain contains a carbohydrate-binding pocket, which binds selectively Manα(1→2)Manα termini in branched high-mannose oligosaccharides. Subtle structural differences between the two pockets result in a slightly higher affinity of domain B for linear di- and trimannosides compared to domain A (*12*, *15*).

CV-N can exist in solution as a monomer as well as a domain-swapped dimer (*16*, *17*) in which two CV-N molecules exchange part of each domain to form a dimeric structure containing four carbohydrate-binding domains, with two A domains comprising residues 1−38/90′−101′ and 1′−38′/90−101, respectively, and two B domains comprising residues 39−50/51′−89′ and 39′−50′/51−89, respectively (*13*, *14*, *18*, *19*). The domain-swapped dimer is a kinetically trapped folding intermediate, and it converts slowly to the thermodynamically stable monomer in physiological conditions, allowing its characterization (*18*, *19*). To date, all of the structures obtained by X-ray crystallography contain the dimer (*13*, *14*, *20*). An analysis of the available structures of the monomer and dimer reveals that a hinge region spanning residues 50−56, which forms a helical turn in the monomer structure, is extended in the dimer to allow the domain swapping (*11*, *14*, *18*, *20*). Mutations in the hinge region can affect significantly the preferential oligomerization state of the protein by affecting the stability of the two forms compared to wt CV-N and their ability to interconvert. For example, Pro51Gly (*18*) is thermodynamically more stable than CV-N in both forms and preferentially exists as a

[†] This work was supported in part by ASU start-up funds (to G.G.) and by the Intramural Research Program of the NIH, National Cancer Institute, Center for Cancer Research.

[‡] PDB accession codes 2PYS and 2Z21.

* To whom correspondence should be addressed. Phone: (480) 965-6645. Fax: (480) 965-2747. E-mail: gghirlanda@asu.edu.

[#] These authors contributed equally to the paper.

[§] Arizona State University.

[||] NCI-Frederick.

[⊥] Current address: Biomedical Research Laboratories, Pharmaceutical Research Division, Takeda Pharmaceutical Co. Ltd., Osaka 532-8686, Japan.

[1] Abbreviations: CV-N, cyanovirin-N; HIV, human immunodeficiency virus.

10.1021/bi700666m CCC: $37.00
Published on Web 07/18/2007

monomer, while Ser52Pro (*18*, *21*) and ΔGln50 (*22*) form exclusively stable domain-swapped dimers.

A possible general model for the interaction between antiviral lectins and viral glycoproteins involving multiple simultaneous binding events, in analogy to other carbohydrate−lectin recognition processes involving multidentate interactions (*23*), is supported by the recent discovery of two lectins unrelated to CV-N with subnanomolar antiviral activity, griffithsin (*24*) and MVL (*25*). These proteins form highly symmetric homodimers, with each monomer containing two independent carbohydrate-binding domains; both proteins bind their oligosaccharide targets, mannose and oligomannosides for griffithsin and the $Man_2GlcNAc_2$ core for MVL, with very high affinity. In cyanovirin, multiple binding interactions with the oligomannoside target could be achieved either by simultaneously engaging both domains A and B in the monomeric form or by engaging two or more binding sites in the domain-swapped dimer form. This hypothesis is further supported by the difference observed in binding linear oligomannosides and glycosylated gp120. While each domain, A and B, binds di- and trimannose independently with dissociation constants in the micromolar range, monomeric CV-N binds gp120 at nanomolar concentrations, suggesting an avidity effect. Some insight into the role of dimerization on the antiviral activity is provided by the hinge region mutants described above: although some variability is observed depending on the specific in vitro assay used, P51G (monomer) and S52P (dimer) appear to have antiviral activity essentially identical to wt CV-N (*18*), while a 3.5 higher activity was observed for ΔQ50 (dimer) (*22*). Conversely, it was shown that mutant CV-Ns in which domain A had been inactivated inhibit HIV-1 envelope-mediated fusion with activity indistinguishable from wt CV-N (*26*). More recently, it was reported that a monomeric domain B knockout mutant, CV-N^{mutDB}, demonstrated complete loss of activity in several antiviral assays (*27*). These results were interpreted as indicating that a functional domain B is necessary for activity, in light of the conserved activity reported for domain A mutants (*26*). However, the domain A knockout mutants contained the native P51 and, consequently, retained the ability to form domain-swapped dimers, thus restoring multivalence.

To clarify the molecular mechanism of action of cyanovirin, we engineered a novel mutant, P51G-m4-CVN, designed to contain a single high-affinity carbohydrate-binding site, domain B, and to fold exclusively as a monomer in physiological conditions. P51G-m4-CVN contains the four mutations in the m4-CVN construct (K3N, T7A, E23I, and N93A) which knock out the carbohydrate-binding ability of domain A (*26*), as well as the hinge region mutation, P51G, which stabilizes the monomer (*18*, *20*). Here, we present the high-resolution crystal structure of P51G-m4-CVN in its free and dimannose-bound form, revealing the first X-ray structure of a CV-N monomer. As designed, the protein contains a single carbohydrate-binding site. The residual carbohydrate-binding site on monomeric P51G-m4-CVN retains its ability to bind one molecule of dimannose with micromolar affinity, in keeping with NMR solution studies of m4-CVN (*26*). Despite a binding affinity for small oligomannosides identical to wild-type CV-N, the binding affinity of our mutant for gp120 is decreased by 2 orders of magnitude, and its antiviral activity is completely abolished. The high-affinity binding to gp120 is recovered in the domain-swapped dimer of P51G-m4-CVN, prepared in extreme conditions (*18*, *20*). Taken together with the extensive literature existing on CV-N and its mutants, the results presented here underscore the importance of multiple independent carbohydrate-binding sites as essential prerequisites for the antiviral activity of CV-N and its derivatives and provide a framework for the design of novel, more potent antiviral proteins.

MATERIALS AND METHODS

Protein Expression and Purification. The synthetic gene of wt CV-N had been cloned previously into a pET26b (+) vector (Novagen) as described (*20*, *37*); the gene contains a C-terminal His tag (6 histidines) separated by a two-residue spacer (Leu Glu). This construct is the starting point for the cloning of m4-CVN and P51G-m4-CVN. To construct m4-CVN and P51G-m4-CVN, four mutations (Lys3Asn, Thr7Ala, Glu23Ile, Asn93Ala) or five mutations (Lys3Asn, Thr7Ala, Glu23Ile, Asn93Ala, and Pro51Gly) were introduced sequentially into the pET (wt CV-N) background using the QuikChange II site-directed mutagenesis kit (Stratagene) with the following forward/reverse primers (GeneTech Biosciences, Tempe, AZ): 5′CCTTGGTAACTTCTCCCAGGCCTGCTACAACTCC/5′GGAGTTGTAGCAGGCCTGGGAGAAGTTACCAAGG (Lys3Asn and Thr7Ala), 5′CCTCCACCTGCATACGTACCAACGGTGGTTAC/5′GTAACCACCGTTGGTACGTATGCAGGTGGAGG (Glu23Ile), 5′GACGACCACATCGCTGCCATCGACGGTACCCTG/5′CAGGGTACCGTCGATGGCAGCGATGTGGTCGTC (Asn93Ala), and 5′GGTTCCCTGAAATGGCAGGGCTCCAACTTCATCGAAACC/5′GGTTTCGATGAAGTTGGAGCCCTGCCATTTCAGGGAACC (Pro51Gly). Each protein (wt CV-N, M4-CVN, P51G-m4-CVN) was expressed in *Escherichia coli* BL-21(DE3) cells and grown at 37 °C in Luria−Bertani (LB) medium. In each case, the cell culture was induced with 1 mM isopropyl β-D-thiogalactoside at an OD_{600} of 0.7 and harvested after 3 h. The cell pellet was lysed by sonication in buffer B (6 M guanidine hydrochloride, 100 mM NaH_2PO_4, 10 mM Tris-HCl, pH 8.0) and clarified by centrifugation as described previously (*19*). The supernatant was purified on a Ni Sepharose fast-flow binding column (Novagen), eluting the protein with 200 mM imidazole under denaturing conditions; pure proteins were obtained with a yield of about 40 mg/L of culture. The proteins in 6 M Gdn were treated with 5 mM DTT (final concentration) and refolded by dialysis against 2 M GdnHCl and 50 mM Tris-HCl, pH 8.0, at room temperature for 6 h and then against 10 mM Tris-HCl, pH 8.0, and 100 mM NaCl overnight at room temperature. The protein was obtained as a pure monomer for P51G-m4-CVN and as a mixture of monomer and dimer for wt CV-N and m4-CVN (see text) and was further purified by gel filtration chromatography. The molecular mass and purity were confirmed using mass spectrometry MALDI-TOF and 16% Tricine SDS−PAGE gel (Invitrogen). Protein concentrations were calculated by measuring tryptophan absorbance in 6 M GdnHCl using an extinction coefficient of 10010 M^{-1} cm^{-1} at 280 nm.

Preparation of the P51G-m4-CVN Dimeric Protein. P51G-m4-CVN dimer was prepared following a protocol similar to that described for dimeric wt CV-N (*20*). Briefly, solutions of monomeric P51G-m4-CVN at high concentration (2 mM

in 10 mM Tris-HCl, pH 8.0) were unfolded by dialysis against 6 M GdnHCl and 10 mM Tris-HCl, pH 8.0, and refolded by extensive dialysis against 10 mM Tris-HCl and 100 mM NaCl, pH 8.0, buffer at room temperature. A large fraction of the P51G-m4-CVN protein precipitated, and aggregates were removed by centrifugation. The refolded protein was concentrated and purified by gel filtration chromatography as described above. Dimer peak fractions were collected and concentrated. The stability over time of the dimer was established by incubating a 7 μM solution of P51G-m4-CVN at 38 °C for 4 days; samples were taken periodically (every hour for the first 12 h; every 2 or 3 h for next 36 h; after 48 h samples were collected every 12 h) and were analyzed by size exclusion chromatography on a Superdex peptide 10/300 GL high-performance column. The monomer and dimer forms were quantified by integrating the elution peaks using QuickStart empower software (Waters Corp., Milford, MA).

Circular Dichroism Spectroscopy. CD spectroscopy experiments were carried out on a Jasco J-1710 spectropolarimeter equipped with a thermostatic cell holder PTC 424S. CD spectra were recorded from 240 to 190 nm in 1 mm cells at protein concentrations of 10−15 μM in 10 mM potassium phosphate, pH 7.0, buffer; the final spectra are the average of three data sets. Thermal unfolding curves were monitored by CD, measuring the molar ellipticity at 200 nm; the sample was heated at rates of 15 or 30 °C/h with a data pitch of 0.5 °C over a temperature range of 10−85 °C. Protein concentrations were determined by measuring tryptophan absorbance in 6 M GdnHCl using an extinction coefficient of 10010 M^{-1} cm^{-1} at 280 nm.

Binding to gp120. Binding of wt CV-N, P51G-m4-CVN, and m4-CVN to glycosylated soluble gp120 was assessed by ELISA as previously described (*1*). Briefly, each well of 96 well plates (Nunc; Maxisorp, Gaithersburg, MD) was incubated with 100 ng of gp120 (rgp 120 HIV-1 MN, baculovirus; ImmunoDiagnostics, Inc.) in PBS at room temperature for 2 h. The plates were washed with PBS containing 0.1% Tween 20 (PBST) three times and blocked with a solution of 3% bovine serum albumin (BSA) overnight at 4 °C. A control plate was incubated with BSA only. After plates were washed three times with PBST, 0.5 log serial dilutions of CV-N, m4-CVN, P51G-m4-CVN monomer, and P51G-m4-CVN dimer to a final concentration in the 0.01 nM to 1 μM range were added to triplicate wells (100 μL per well) and incubated for 1 h. The plates were washed with PBST and incubated with anti-CV-N rabbit polyclonal antibody (1:1000 dilution; final concentration 10 μg/mL) for 1 h, washed again with PBST, and incubated with secondary anti-rabbit IgG antibodies conjugated to horseradish peroxidase (Sigma, St. Louis, MO). After 1 h the plates were washed with PBST, and 100 μL of tetramethylbenzidine peroxidase substrate (Kirkegaard & Perry Laboratories, Gaithersburg, MD) was added to each well. After incubation for approximately 2 min, the absorbance at 650 nm was recorded. The reaction was stopped with 50 μL of 2 M H_2SO_4, and the absorbance at 450 nm was read.

Anti-HIV Activity Assay. Anti-HIV activity of CV-N and P51G-m4-CVN proteins was studied using a modified XTT assay (*36*). Serial dilutions of 100 μL of CV-N or P51G-m4-CVN were added to 50 μL of human lymphocyte CEM-SS (1×10^5cells/mL) on 96-well plates. Cells were infected with 50 μL of HIV-1_{RF} virus. Plates were incubated for 6 days at 37 °C and stained with XTT. Metabolic reduction of tetrazolium salt XTT to colored formazan was measured at 450 nm to determine cellular viability. Virus uninfected cells reduce XTT to a soluble formazan and HIV-infected cells cannot reduce XTT.

Crystallization. Initial screening for crystallization conditions was performed using 1536 conditions at the high-throughput screening facility at Hauptman-Woodward Medical Institute (Buffalo, NY). Conditions forming small crystals were selected and optimized at Arizona State University in a hanging drop assay (Linbro plates; Hampton Research). After optimization, the best crystals were observed using vapor diffusion; 100 mM HEPES, pH 6, 100 mM Mg_2SO_4, and 30% (w/v) PEG 8000 as precipitant in the reservoir buffer were equilibrated against a 2−5 μL drop of a 1:1 mixture of 10 mg/mL protein in water and reservoir buffer.

Crystals of the sugar complex were obtained in the same conditions in the presence of 2 mM Man_2. The crystals were harvested directly from the coverslip and flash frozen in liquid nitrogen. The diffraction pattern of the crystals was measured with an in-home X-ray source Rigaku RGB 200 with a Raxis IV++ detector. The software used for data collection was Crystal Clear (*38*). For the primary data evaluation of X-ray data we used the software package HKL 2000 version 1.93 (*39*, *40*). The indexed and scaled data were further evaluated with the software kit CCP4i (*38*). The starting model for molecular replacement was PDB 1LOM divided in the 1−51 and 52−101 parts of the protein. The program Phaser 1.3.1 (*41*) was used for molecular replacement. The calculated model from Phaser was then input to ARP/wARP version 6.0 (*42*, *43*) for further improvement. Final refinement was made manually with XtalView (*44*) and several rounds of Refmac 5.2.0019 (*45*).

RESULTS

Crystal Structure of P51G-m4-CVN. The crystal structure of P51G-m4-CVN was solved at 1.8 Å resolution by molecular replacement (Figure 1), using the structure of segments 1−51 and 52−101 of a mutant domain-swapped form [P51S, S52P; PDB accession number 1LOM (*28*)] as a starting model, as described in the Materials and Methods section. The free form of P51G-m4-CVN and its complex with Manα(1→2)Manα crystallized in similar conditions, yielding crystals of the monoclinic space group $P2_1$ and with similar cell parameters. The crystallographic statistics are reported in Table 1; both crystal forms contain two monomers in the asymmetric unit (Figure 2).

The two monomers are oriented approximately parallel, with a 120° rotation with respect to each other; this spatial arrangement is completely distinct from the one observed in the domain-swapped structures. The Cα backbone rmsd between the two monomers is about 0.5 Å. The structures are well refined, with *R*-factors of 16.5% and 16.4% and R_{free} values of 21.5% and 23.5%, respectively, for the dimannose-bound and the free form. Comparison of the free and dimannose-bound form reveals that binding to Manα-(1→2)Manα does not lead to significant conformational changes in the position of the backbone atoms.

Overall, the structure of P51G-m4-CVN is remarkably similar to that of wt CV-N (Figure 1); an overlay of the two

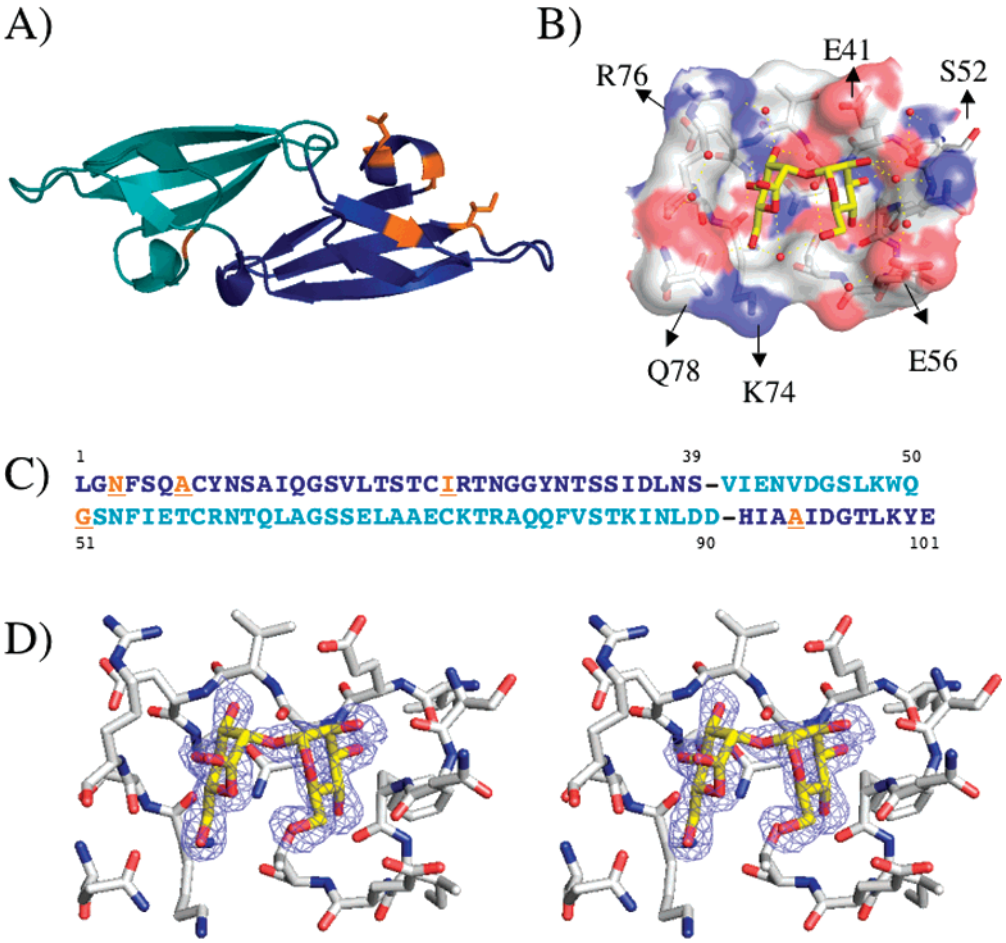

FIGURE 1: Crystal structure of free P51G-m4-CVN at 1.8 Å resolution. The coordinates of the free protein (PDB accession code 2Z21) and of the complex with Manα(1→2)Man (PDB accession number 2PYS) overlay with a rmsd of less than 0.3 Å; in both crystal forms, two molecules are found in the unit cell, oriented parallel but rotated by 120° to each other. Panel A: Ribbon diagram of one monomer from the structure of the free protein. Domain B (cyan), spanning residues 39−89, is unaltered from wt CV-N, while domain A (residues 1−38 and 90−101, blue) contains four mutations in the binding site (K3N, T7A, E23I, N93A) in addition to the P51G mutation in the hinge region. The mutated residues are highlighted in orange. Panel B: Detail of the carbohydrate-binding pocket. Side chains involved in binding are represented in sticks and colored by atom (carbon, green; oxygen, red; nitrogen, blue); dimannose is represented in sticks and colored by atom (carbon, yellow; oxygen, red), and crystallographic water molecules are represented as red spheres; direct or water-mediated hydrogen bonds are indicated by dashed lines. Panel C: Sequence of P51G-m4-CVN, with domain B in cyan and domain A in dark blue. Mutations from wt are in orange. Panel D: Detail of the carbohydrate-binding pocket (stereoview) color coded as in panel B. The omit electron density map of the sugar-binding pocket, generated using SFCHECK (*29*), is depicted as mesh plotted at a contrast level of 1σ. This figure was generated with MacPyMol (*30*).

structures, using the solution structure of monomeric wt CV-N bound to two molecules of Manα (1→2)Manα [PDB accession code 1IIY) (*12*)], reveals a Cα backbone rmsd of 0.8 Å. The main deviation in the backbone atom position is observed between the hinge region (residues 50−52) that connects domains A and B. The structure of the dimannose-bound P51G-m4-CVN reveals the molecular details of the binding pocket (Figure 1B,D). Compared with the NMR structure of wt CV-N, the position of the backbone atoms in the remaining unique sugar-binding pocket (domain B) is conserved, with minimal differences observed in the position of the hairpin loop corresponding to residues 74−79. Molecular dynamics studies had predicted a high flexibility at this site (*31*); however, the sugar-binding site in our structure is very well defined as indicated by low *B* factors. The bound dimannose [Manα(1→2)Manα] in domain B occupies slightly different conformations than observed in the NMR structure (*12*), as reflected by different values of the glycosidic dihedral angles Ψ and Φ (*31*): in 1IIY, the angles are 36.9° and −48.43°, respectively, while in our crystal structure we observe a Ψ value of 30.98° and a Φ value of −26.6°. Both sets of values are in the lowest free energy region in glycosidic dihedral space, centered at$\Phi = -40°$ and $\Psi = 40°$ (*31*). The position of the side chains and backbone polar atoms lining the cavity and making hydrogen bonds with the dimannose is also conserved, with the exception of Arg 76. In the NMR structure, Arg 76 assumes a side chain conformation that allows the formation of two hydrogen bonds with the bound dimannose, thus locking the sugar in place; this mechanism has been supported by molecular dynamics simulations (*31*). In contrast, we observe a different side chain rotamer of Arg 76, in which hydrogen bonding to the sugar is mediated by a water molecule. Our structural data support an inherent flexibility of the binding site, which can accommodate slightly different conformations, thereby explaining the ability of cyanovirin to recognize several related high-mannose glycans. In addition, glycan microarray studies have shown some binding to lacto and neolacto structures (*32*).

Table 1: Crystallographic Data Collection Statistics

	P51G-m4-CVN with dimannose (Man_2)	P51G-m4-CVN
unit cell parameters		
a, *b*, *c* (Å)	49.23, 38.28, 55.79	49.46, 38.14, 56.04
α, *β*, *γ* (deg)	90, 99.69, 90	90, 99.98, 90
space group	$P2_1$	$P2_1$
molecules/ asymmetric unit	2	2
resolution (Å)	1.8−55.2 (1.8−10)[b]	1.8−31.4
unique reflections	18274 (17236)[b]	16958 (16077)[b]
completeness (%)	94.8 (82.33)[a]	87.7 (42.3)[a]
R-factor	0.169	0.164
R_{free}	0.215	0.235
R_{merge}	9.4 (42.0)[a]	9.4 (24.4)[a]
data redundancy	2.8 (2.6)[a]	1.9 (1.4)[a]
bonds (Å)	0.017	0.011
angles (deg)	1.733	1.23
dihedrals (deg)	29.6	29.6
mean *B*-value (Å^2)	22.5	23.5
I/σ	8.87 (2.93)[a]	11.5 (3.7)[a]
solvent (%)	43.5	43.5
PDB code	2PYS	2Z21

[a] The numbers in parentheses refer to the higher resolution bin (1.8−1.85 for 2PYS and 1.8−1.84 for 2Z21). [b] Used for refinement.

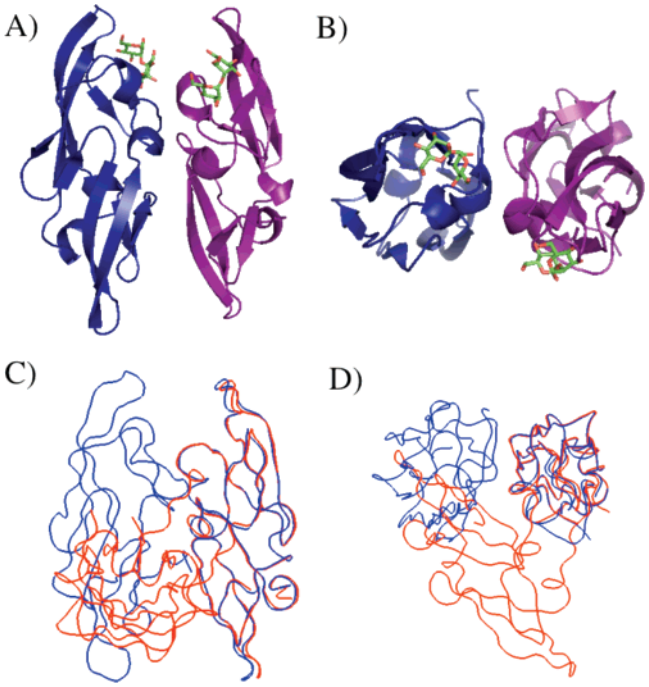

FIGURE 2: Crystal structure of P51G-m4-CVN. Two molecules are found in the asymmetric unit. Panels A (side view) and B (top view): Ribbon diagram of the crystallographic dimer in complex with Man_2. One monomer is represented in blue and the other in magenta, while the sugar is represented in sticks and colored by atom (carbon, green; oxygen, red). Panels C and D show an overlay of the backbone atoms of the crystallographic dimer of P51G-m4-CVN (blue) and of the domain-swapped dimer of wt CV-N (red) [PDB code 1M5J (*12*)].

P51G-m4-CVN Is a Monomer in Solution. Recombinant wt CV-N exists in solution in multiple aggregation states: when expressed in *E. coli*, purified, and refolded from inclusion bodies using standard protocols, wt CV-N exhibits a gel filtration elution profile with two major peaks corresponding to the monomer (main peak) and the dimer and smaller peaks corresponding to higher order aggregates (*20*). The low-affinity binding site knockout, m4-CVN (*26*),

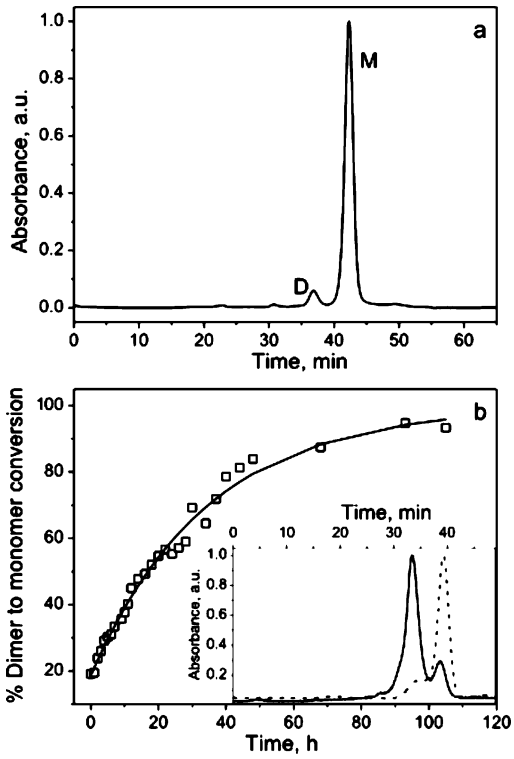

FIGURE 3: Size exclusion chromatography. (a) P51G-m4-CVN elution profile monitored at 280 nm in 10 nM potassium phosphate, pH 7.), shows a minor peak (approximately 3% of the total protein) for the dimeric form, and a major peak corresponding to the monomeric form of the protein. (b) Time course of P51G-m4-CVN dimer conversion to monomer. 7 μM dimer protein in 10 mM potassium phosphate, pH 7.0, was incubated at 38 °C and analyzed by size exclusion chromatography. The percentage of monomer and dimer forms was determined by integrating the area under each elution peak. The insert shows the elution profile of the P51G-m4-CVN dimer after 1 h incubation at 38 °C (solid line) and after 93 h incubation at 38 °C (dashed line).

exhibits a similar behavior, eluting in two main peaks corresponding to the monomer and the dimer and accounting for approximately 60% and 40% of the total protein, respectively (data not shown). In contrast, the elution profile of recombinant P51G-m4-CVN purified in similar conditions exhibits a single major peak at 42 min, corresponding to the monomeric form, which accounts for 97% of the total protein; a minor peak at 38 min, accounting for approximately 3% of the total protein, corresponds to the dimer (Figure 3a). A similar behavior had been observed for the hinge region mutant P51G-CVN (*21*).

The domain-swapped dimer of P51G-m4-CVN can be prepared by partially unfolding and refolding the monomer at high concentrations, as previously observed with wt CV-N and P51G-CVN (*18*, *20*); the mixture of monomer and dimer can be separated by gel filtration chromatography (see Materials and Methods section). Similarly to wt CV-N (*20*), the dimer is a metastable form and converts to monomer upon incubation of low micromolar solutions at the temperature (38 °C) used for antiviral activity assays. The process was monitored by gel filtration chromatography over a period of several days (Figure 3b): at equilibrium, over 95% of the dimer has reverted to monomer with an estimated half-life of about 20 h. Conversely, the monomer does not convert appreciably to the dimer upon prolonged incubation at 38 °C at concentrations ranging between 10 and 50 μM. For

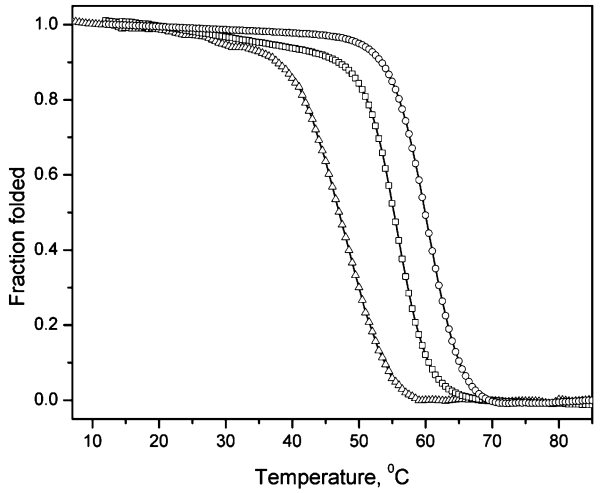

FIGURE 4: Thermal denaturation profiles of P51G-m4-CVN (circles), m4-CVN (triangles), and wt CV-N (squares). The corresponding melting points are 62, 45, and 58 °C, respectively. The unfolding transitions were monitored at 200 nm in the 10−85 °C range. All measurements were carried out at protein concentrations of 10−15 μM in 10 mM potassium phosphate, pH 7.0, buffer.

comparison, dimeric wt CV-N converts to its monomeric form at 38 °C with a half-life of approximately 12 h (*20*).

These observations are consistent with the stabilization of the monomeric form observed for the P51G mutant relative to wt CV-N; as expected, the hinge mutation has a similar effect on the m4-CVN mutant background.

Thermodynamic Stability. P51G-m4-CVN exhibits a circular dichroism (CD) spectrum typical of mainly β structures and identical to that of CV-N (data not shown), with a minimum at 212 nm and maximum at 190 nm (*33*). The thermodynamic stability of P51G-m4-CVN was assessed by thermal denaturation, monitoring the loss of secondary structure at increasing temperatures from 5 to 95 °C by CD at 200 nm, where the largest change is observed between folded and unfolded spectra. The thermal denaturation profiles of wt CV-N, m4-CVN, and P51G-m4-CVN are shown in Figure 4. The four mutations introduced in m4-CVN significantly destabilize the protein: the melting temperature is lowered by about 12 °C from 58 °C for wt CV-N to 46 °C. On the other end, the additional Pro51Gly mutation in P51G-m4-CVN increases the T_m to approximately 62 °C. This result was not unexpected, as the single point [P51G]-CV-N mutant is significantly more stable than wt CV-N (*21*). Thus, the conflicting effect of the two groups of mutations introduced appears to compensate each other, resulting in slightly increased stability of P51G-m4-CVN compared to wt CV-N.

Binding to gp120 Is Modulated by the Oligomerization State. The direct interaction of P51G-m4-CVN monomer and dimer with the viral surface glycoprotein gp120 was measured in an ELISA experiment; the relative binding was compared to wt CV-N and m4-CVN. The results are shown in Figure 5; surprisingly, binding of P51G-m4-CVN to gp120 is strongly dependent on the oligomerization state of the protein. A dramatic shift of 2 orders of magnitudes is seen between the affinity of dimeric P51G-m4-CVN, which has a EC_{50} of 0.8 nM, and monomeric P51G-m4-CVN, which has a EC_{50} of approximately 80 nM. In comparison, wt CV-N monomer binds to gp120 with high affinity (EC_{50} of approximately 0.12 nM), similarly to the results previously

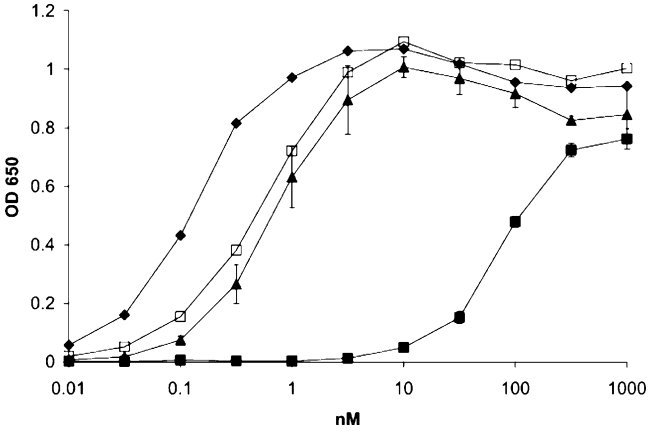

FIGURE 5: ELISA study of the binding of CV-N, m4-CVN, P51G-m4-CVN monomer, and P51G-m4-CVN dimer to gp120. Serial dilutions of proteins were added to plates covered with 100 ng per well of native gp120 [CVN (diamonds), m4-CVN (triangles), P51G-m4-CVN dimer (open squares), or P51G-m4-CVN monomer (closed squares)]. In all cases polyclonal rabbit anti-CVN antibodies were used to detect the bound proteins followed by incubation with anti-rabbit IgG−peroxidase antibodies; the peroxidase-catalyzed oxidation of TMB was monitored at 650 nm. All data were corrected for background, and the data points represent averages ± standard deviations of triplicate determinations. The response curves indicate saturable binding interactions for all mutants.

reported (*33*, *34*), while m4-CVN monomer binds with slightly weaker affinity (EC_{50} of approximately 0.6 nM). Thus, the remarkable decrease in binding affinity observed for monomeric P51G-m4-CVN cannot be simply attributed to the impairment of domain A: the strong binding observed for m4-CVN indicates that the residual domain B is capable of binding gp120 with a level of function comparable to wt CV-N. This result is consistent with previous NMR measurements indicating that domain B in m4-CVN binds dimannose with affinity identical to domain B in wt CV-N (*26*). The difference in binding between monomeric P51G-m4-CVN and m4-CVN implicates a role of the hinge region mutation, [P51G], which increases the free energy barrier for the interconversion of the monomer and dimer. Thus, the monomer P51G-m4-CVN, which contains a single mannose-binding domain and is unable to convert to dimer, interacts inefficiently with gp120. This hypothesis is supported by the recovery of binding affinity observed in the dimeric form of P51G-m4-CVN.

The P51G-m4-CVN Monomer Is Inactive against HIV. The type of assay used to assess the antiviral activity of CV-N and its mutants and the experimental conditions each assay requires affect the results obtained. For example, dimeric wt CV-N is about 3.5-fold more active than its monomer in a quantitative cell fusion assay based on vaccinia virus (*22*, *35*), yet these results could not be replicated in cellular assays, which measure cellular viability after exposure to HIV in the presence of the antiviral agent of interest. These assays are complicated by the time scale of the dimer−monomer conversion at 38 °C, which prevents a direct test of dimeric CV-N utilizing the XXT-tetrazolium assay (*18*, *20*), due to lengthy incubations of several days at physiological temperature. Similar cellular assays on monomeric (P51G) and dimeric (ΔQ50) hinge mutants of CV-N, stable in the assay conditions, showed indistinguishable activity (*18*).

Table 2: Anti-HIV Activity of CV-N, m4-CVN, and P51G-m4-CVN Monomer

mutant	EC_{50} (nM)
CV-N (wt)	0.9
m4-CVN	240
P51G-m4-CVN	undetermined (≫1000)

The anti-HIV activity of monomeric P51G-m4-CVN was assessed using the XTT-tetraxolium assay (*36*); in parallel, wt CV-N and m4-CVN were tested as a comparison. Dimer P51G-m4-CVN was not included in the test due to its conversion to monomer in the time frame of the experiment. The results are shown in Table 2.

While wt CV-N was active at low nanomolar concentrations (EC_{50} approximately 0.9 nM), in accordance to literature data (*21*), m4-CVN exhibited similar activity at significantly higher concentrations (EC_{50} of approximately 0.24 μM). P51G-m4-CVN showed no activity at concentrations as high as 1 μM.

The reduced activity of m4-CVN compared to wt CV-N is surprising: m4-CVN inhibits HIV-1 envelope-mediated cell fusion (*35*) with activity nearly identical to that of monomeric wt CV-N (*26*). The inactivation observed with a cellular assay, which requires longer incubations at 38 °C (a week compared with a few hours for the cell fusion assay), might be due to its reduced thermal stability, which might lead to its partial denaturation at the assay conditions. However, this explanation could not be extended to P51G-m4-CVN, which is significantly more stable than wt CV-N to thermal denaturation. In this mutant, the complete loss of antiviral function observed for the monomer contrasts sharply with the decrease observed for m4-CVN and points to a role of the hinge region mutation. Similarly to what is observed for binding to gp120, the presence of two or more mannose-binding domains on a single monomer, or the ability to form domain-swapped dimers, appears to be crucial for function. In support of this hypothesis, results from different groups show an increased anti-HIV activity of domain-swapped dimers of CV-N in assays requiring only brief incubations at 38 °C (*22*), compatible with significant concentrations of dimers, while cellular assays requiring longer incubations at 38 °C, during which the dimers are known to convert to monomers, show identical activities (*18*).

DISCUSSION

In this work, we present the crystal structure of P51G-m4-CVN, a monomeric mutant of CV-N, as well as its thermodynamic properties, binding affinity to gp120, and anti-HIV activity as a function of its oligomerization state. A hinge region mutation (P51G) in P51G-m4-CVN stabilizes the monomeric form and hampers its conversion to dimer, while mutations in domain A abolish one of the two carbohydrate-binding sites. The remaining site on domain B is unaltered in the mutant and is fully functional. The high-resolution crystal structures of P51G-m4-CVN in its free and dimannose-bound form contain the monomeric fold previously observed only by NMR. The molecular detail of dimannose bound to domain B reveals a unique mode of binding.

Surprisingly, P51G-m4-CVN shows a 700-fold decrease in its affinity for soluble gp120. Moreover, the protein's ability to protect cells from HIV infection is completely abolished. These effects cannot be simply attributed to the inactivation of domain A: m4-CVN, a domain A knockout mutant previously described (*26*), which retains the wt ability to form domain swapped dimers, binds gp120 with only a 4-fold decreased affinity compared to wt CV-N (Figure 5) and shows significant anitviral activity in cellular assays. Furthermore, high-affinity binding to gp120 comparable to wt CV-N and m4-CVN was restored in P51G-m4-CVN by forcing the formation of the domain-swapped dimer in nonphysiological conditions; the dimeric P51G-m4-CVN contains two carbohydrate-binding domains per molecule.

The relationship between oligomerization state, binding to gp120, and antiviral activity is a complex one (*18*). Several factors are involved, including the relative stability of the proteins and the type of antiviral assay used. Our observation that monomeric P51G-m4-CVN has no antiviral activity at the concentrations tested, despite its increased stability compared to wt CV-N, supports the hypothesis that multisite binding is crucial for the antiviral activity of CV-N. The identity of the binding sites on CV-N and its mutants does not seem to be as relevant: recent work on a monomeric domain B knockout mutant, CV-N^{mutDB}, demonstrated its complete loss of activity in several antiviral assays (*27*). While this was interpreted to indicate that oligomannose binding via domain B is essential for activity (*27*), the additional data presented here suggest that the identiy of the residual carbohydrate binding domain, A or B, is not as important for activity as the ability to form multiple protein−oligomannoside interactions on the surface of gp120. In wt CV-N, the monomer contains two binding domains, which can be augmented to four in the domain-swapped dimer. In mutants containing only one domain per monomer, multiple interactions can only be achieved via formation of the dimer. In this context, the equilibrium between monomer and dimer becomes crucial; although this process has been characterized only in solution, it is not clear whether the presence of high local concentrations of oligomannosides on gp120 could have an effect on the equilibrium, perhaps stabilizing the domain-swapped dimer. This process would be hampered in mutants containing the [P51G] substitution, which has been shown to slow the equilibration of the two forms and further stabilizes the monomer (*18*).

In this report we showed that the presence of a single carbohydrate-binding domain in the monomeric form of cyanovirin is not sufficient for high-affinity binding to gp120 and leads to the loss of the antiviral activity. Interpreted in light of the results obtained by other groups on CV-N and its mutants, these data corroborate a general mechanism of action for antiviral lectins based on multivalent binding to the target oligosaccharides on the surface of envelope glycoproteins.

ACKNOWLEDGMENT

We gratefully acknowledge the Hauptman-Woodward Medical Institute for high-throughput screening of crystallization conditions for P51G-m4-CVN. We thank Angela Gronenborn for preliminary HSQC NMR experiments and for helpful discussions and Roberta S. Gardella for technical assistance with the HIV test.

REFERENCES

1. Boyd, M. R., Gustafson, K. R., McMahon, J. B., Shoemaker, R. H., O'Keefe, B. R., Mori, T., Gulakowski, R. J., Wu, L., Rivera, M. I., Laurencot, C. M., Currens, M. J., Cardellina, II, J. H., Buckheit, R. W., Jr., Nara, P. L., Pannell, L. K., Sowder, R. C., II, and Henderson, L. E. (1997) Discovery of cyanovirin-N, a novel human immunodeficiency virus-inactivating protein that binds viral surface envelope glycoprotein gp120: potential applications to microbicide development, *Antimicrob. Agents Chemother. 41*, 1521−1530.
2. O'Keefe, B. R., Smee, D. F., Turpin, J. A., Saucedo, C. J., Gustafson, K. R., Mori, T., Blakeslee, D., Buckheit, R., and Boyd, M. R. (2003) Potent anti-influenza activity of cyanovirin-N and interactions with viral hemagglutinin, *Antimicrob. Agents Chemother. 47*, 2518−2525.
3. Helle, F., Wychowski, C., Vu-Dac, N., Gustafson, K. R., Voisset, C., and Dubuisson, J. (2006) Cyanovirin-N inhibits hepatitis C virus entry by binding to envelope protein glycans, *J. Biol. Chem. 281*, 25177−25183.
4. Barrientos, L. G., and Gronenborn, A. M. (2005) The highly specific carbohydrate-binding protein cyanovirin-N: structure, anti-HIV/Ebola activity and possibilities for therapy, *Mini Rev. Med. Chem. 5*, 21−31.
5. De Clercq, E. (2005) Emerging anti-HIV drugs, *Expert Opin. Emerg. Drugs 10*, 241−273.
6. Reeves, J. D., and Piefer, A. J. (2005) Emerging drug targets for antiretroviral therapy, *Drugs 65*, 1747−1766.
7. Dey, B., Lerner, D. L., Lusso, P., Boyd, M. R., Elder, J. H., and Berger, E. A. (2000) Multiple antiviral activities of cyanovirin-N: blocking of human immunodeficiency virus type 1 gp120 interaction with CD4 and coreceptor and inhibition of diverse enveloped viruses, *J. Virol. 74*, 4562−4569.
8. Esser, M. T., Mori, T., Mondor, I., Sattentau, Q. J., Dey, B., Berger, E. A., Boyd, M. R., and Lifson, J. D. (1999) Cyanovirin-N binds to gp120 to interfere with CD4-dependent human immunodeficiency virus type 1 virion binding, fusion, and infectivity but does not affect the CD4 binding site on gp120 or soluble CD4-induced conformational changes in gp120, *J. Virol. 73*, 4360−4371.
9. Barrientos, L. G., O'Keefe, B. R., Bray, M., Sanchez, A., Gronenborn, A. M., and Boyd, M. R. (2003) Cyanovirin-N binds to the viral surface glycoprotein, GP1,2 and inhibits infectivity of Ebola virus, *Antiviral Res. 58*, 47−56.
10. Botos, I., and Wlodawer, A. (2003) Cyanovirin-N: a sugar-binding antiviral protein with a new twist, *Cell. Mol. Life Sci. 60*, 277−287.
11. Bewley, C. A., Gustafson, K. R., Boyd, M. R., Covell, D. G., Bax, A., Clore, G. M., and Gronenborn, A. M. (1998) Solution structure of cyanovirin-N, a potent HIV-inactivating protein, *Nat. Struct. Biol. 5*, 571−578.
12. Bewley, C. A. (2001) Solution structure of a cyanovirin-N:Man alpha 1−2Man alpha complex: structural basis for high-affinity carbohydrate-mediated binding to gp120, *Structure (Cambridge) 9*, 931−940.
13. Botos, I., O'Keefe, B. R., Shenoy, S. R., Cartner, L. K., Ratner, D. M., Seeberger, P. H., Boyd, M. R., and Wlodawer, A. (2002) Structures of the complexes of a potent anti-HIV protein cyanovirin-N and high mannose oligosaccharides, *J. Biol. Chem. 277*, 34336−34342.
14. Yang, F., Bewley, C. A., Louis, J. M., Gustafson, K. R., Boyd, M. R., Gronenborn, A. M., Clore, G. M., and Wlodawer, A. (1999) Crystal structure of cyanovirin-N, a potent HIV-inactivating protein, shows unexpected domain swapping, *J. Mol. Biol. 288*, 403−412.
15. Shenoy, S. R., Barrientos, L. G., Ratner, D. M., O'Keefe, B. R., Seeberger, P. H., Gronenborn, A. M., and Boyd, M. R. (2002) Multisite and multivalent binding between cyanovirin-N and branched oligomannosides: calorimetric and NMR characterization, *Chem. Biol. 9*, 1109−1118.
16. Liu, Y., and Eisenberg, D. (2002) 3D domain swapping: as domains continue to swap, *Protein Sci. 11*, 1285−1299.
17. Bennett, M. J., Choe, S., and Eisenberg, D. (1994) Domain swapping: entangling alliances between proteins, *Proc. Natl. Acad. Sci. U.S.A. 91*, 3127−3131.
18. Barrientos, L. G., Lasala, F., Delgado, R., Sanchez, A., and Gronenborn, A. M. (2004) Flipping the switch from monomeric to dimeric CV-N has little effect on antiviral activity, *Structure (Cambridge) 12*, 1799−1807.
19. Barrientos, L. G., and Gronenborn, A. M. (2002) The domain-swapped dimer of cyanovirin-N contains two sets of oligosaccharide binding sites in solution, *Biochem. Biophys. Res. Commun. 298*, 598−602.
20. Barrientos, L. G., Louis, J. M., Botos, I., Mori, T., Han, Z., O'Keefe, B. R., Boyd, M. R., Wlodawer, A., and Gronenborn, A. M. (2002) The domain-swapped dimer of cyanovirin-N is in a metastable folded state: reconciliation of X-ray and NMR structures, *Structure 10*, 673−686.
21. Mori, T., Barrientos, L. G., Han, Z., Gronenborn, A. M., Turpin, J. A., and Boyd, M. R. (2002) Functional homologs of cyanovirin-N amenable to mass production in prokaryotic and eukaryotic hosts, *Protein Expression Purif. 26*, 42−49.
22. Kelley, B. S., Chang, L. C., and Bewley, C. A. (2002) Engineering an obligate domain-swapped dimer of cyanovirin-N with enhanced anti-HIV activity, *J. Am. Chem. Soc. 124*, 3210−3211.
23. Bertozzi, C. R., and Kiessling, L. L. (2001) Chemical glycobiology, *Science 291*, 2357−2364.
24. Ziolkowska, N. E., O'Keefe, B. R., Mori, T., Zhu, C., Giomarelli, B., Vojdani, F., Palmer, K. E., McMahon, J. B., and Wlodawer, A. (2006) Domain-swapped structure of the potent antiviral protein griffithsin and its mode of carbohydrate binding, *Structure 14*, 1127−1135.
25. Williams, D. C., Jr., Lee, J. Y., Cai, M., Bewley, C. A., and Clore, G. M. (2005) Crystal structures of the HIV-1 inhibitory cyanobacterial protein MVL free and bound to Man3GlcNAc2: structural basis for specificity and high-affinity binding to the core pentasaccharide from N-linked oligomannoside, *J. Biol. Chem. 280*, 29269−29276.
26. Chang, L. C., and Bewley, C. A. (2002) Potent inhibition of HIV-1 fusion by cyanovirin-N requires only a single high affinity carbohydrate binding site: characterization of low affinity carbohydrate binding site knockout mutants, *J. Mol. Biol. 318*, 1−8.
27. Barrientos, L. G., Matei, E., Lasala, F., Delgado, R., and Gronenborn, A. M. (2006) Dissecting carbohydrate-cyanovirin-N binding by structure-guided mutagenesis: functional implications for viral entry inhibition, *Protein Eng., Des. Sel. 19*, 525−535.
28. Botos, I., Mori, T., Cartner, L. K., Boyd, M. R., and Wlodawer, A. (2002) Domain-swapped structure of a mutant of cyanovirin-N, *Biochem. Biophys. Res. Commun. 294*, 184−190.
29. Vaguine, A. A., Richelle, J., and Wodak, S. J. (1999) SFCHECK: a unified set of procedures for evaluating the quality of macromolecular structure-factor data and their agreement with the atomic model, *Acta Crystallogr., Sect. D: Biol. Crystallogr. 55*, 191−205.
30. Delano, W. L. (2005) Delano Scientific, LLC, South San Francisco, CA.
31. Margulis, C. J. (2005) Computational study of the dynamics of mannose disaccharides free in solution and bound to the potent anti-HIV virucidal protein cyanovirin, *J. Phys. Chem. B 109*, 3639−3647.
32. Blixt, O., Head, S., Mondala, T., Scanlan, C., Huflejt, M. E., Alvarez, R., Bryan, M. C., Fazio, F., Calarese, D., Stevens, J., Razi, N., Stevens, D. J., Skehel, J. J., van Die, I., Burton, D. R., Wilson, I. A., Cummings, R., Bovin, N., Wong, C. H., and Paulson, J. C. (2004) Printed covalent glycan array for ligand profiling of diverse glycan binding proteins, *Proc. Natl. Acad. Sci. U.S.A. 101*, 17033−17038.
33. Barrientos, L. G., Louis, J. M., Hung, J., Smith, T. H., O'Keefe, B. R., Gardella, R. S., Mori, T., Boyd, M. R., and Gronenborn, A. M. (2002) Design and initial characterization of a circular permuted variant of the potent HIV-inactivating protein cyanovirin-N, *Proteins 46*, 153−160.
34. O'Keefe, B. R., Shenoy, S. R., Xie, D., Zhang, W., Muschik, J. M., Currens, M. J., Chaiken, I., and Boyd, M. R. (2000) Analysis of the interaction between the HIV-inactivating protein cyanovirin-N and soluble forms of the envelope glycoproteins gp120 and gp41, *Mol. Pharmacol. 58*, 982−992.
35. Nussbaum, O., Broder, C. C., and Berger, E. A. (1994) Fusogenic mechanisms of enveloped-virus glycoproteins analyzed by a novel recombinant vaccinia virus-based assay quantitating cell fusion-dependent reporter gene activation, *J. Virol. 68*, 5411−5422.
36. Gulakowski, R. J., McMahon, J. B., Staley, P. G., Moran, R. A., and Boyd, M. R. (1991) A semiautomated multiparameter approach for anti-HIV drug screening, *J. Virol. Methods 33*, 87−100.
37. Mori, T., Gustafson, K. R., Pannell, L. K., Shoemaker, R. H., Wu, L., McMahon, J. B., and Boyd, M. R. (1998) Recombinant

production of cyanovirin-N, a potent human immunodeficiency virus-inactivating protein derived from a cultured cyanobacterium, *Protein Expression Purif. 12*, 151−158.
38. Collaborative Computational Project, Number 4 (1994) The CCP4 Suite−Programs for Protein Crystallography, *Acta Crystallogr., Sect. D: Biol. Crystallogr. 50*, 760−763.
39. Minor, W., Cymborowski, M., Otwinowski, Z., and Chruszcz, M. (2006) HKL-3000: the integration of data reduction and structure solution−from diffraction images to an initial model in minutes, *Acta Crystallogr., Sect. D: Biol. Crystallogr. 62*, 859−866.
40. Otwinowski, Z., and Minor, W. (1997) Processing of X-ray diffraction data collected in oscillation mode, *Macromol. Crystallogr., Part A 276*, 307−326.
41. McCoy, A. J., Grosse-Kunstleve, R. W., Storoni, L. C., and Read, R. J. (2005) Likelihood-enhanced fast translation functions, *Acta Crystallogr., Sect. D: Biol. Crystallogr. 61*, 458−464.
42. Perrakis, A., Morris, R., and Lamzin, V. S. (1999) Automated protein model building combined with iterative structure refinement, *Nat. Struct. Biol. 6*, 458−463.
43. Perrakis, A., Harkiolaki, M., Wilson, K. S., and Lamzin, V. S. (2001) ARP/wARP and molecular replacement, *Acta Crystallogr., Sect. D: Biol. Crystallogr. 57*, 1445−1450.
44. McRee, D. E. (1999) XtalView Xfit−A versatile program for manipulating atomic coordinates and electron density, *J. Struct. Biol. 125*, 156−165.
45. Murshudov, G. N., Vagin, A. A., and Dodson, E. J. (1997) Refinement of macromolecular structures by the maximum-likelihood method, *Acta Crystallogr., Sect. D: Biol. Crystallogr. 53*, 240−255.

BI700666M